[Short title + Author Name - P&H title] 17 (2024) 105396

Contents lists available at ScienceDirect

Arabian Journal of Chemistry

journal homepage: www.ksu.edu.sa

The synthesis of new non-ionic surfactant 1-(2, 4-dinitrophenyl)-3-dodecanoylthiourea: An efficient candidate for drug deliveries and metabolism processes

Amjad Ali [a,b,c], Ahmad Naveed [a,*], Imdad Ali [d], Muhammad Suleman [e], Sofia Nosheen [f], Saira manzoor [g], Tariq Aziz [h], Jamile Mohammadi Moradian [a], Suliman Yousef Alomar [i], Li Guo [a,*]

[a] Research School of Polymeric Materials, School of Materials Science and Engineering, Jiangsu University, Zhenjiang 212013, China
[b] Institute of Chemistry, University of Silesia, Szkolna 9, Katowice 40-600, Poland
[c] MOE Key Laboratory of Macromolecular Synthesis and Functionalization, Department of Polymer Science and Engineering, Zhejiang University, Hangzhou 310027, China
[d] H.E.J. Research Institute of Chemistry, International Centre for Chemical and Biological Sciences, University of Karachi, Karachi 74200, Pakistan
[e] Department of Chemistry Zhejiang University, Hangzhou 310027, China
[f] Department of Environmental Science, Lahore college for Women University, Lahore, Pakistan
[g] Institute of Microscale Optoelectronics, Shenzhen University, Shenzhen 518060, China
[h] Faculty of Civil Engineering and Mechanics, Jiangsu University, Zhenjiang 212013, China
[i] Zoology Department, College of Science, King Saud University, Riyadh 11451, Saudi Arabia

ARTICLE INFO

Keywords:
Surfactant
Electrochemical
Drug deliveries
Metabolism

ABSTRACT

By utilizing the reaction of lauryl chloride, potassium thiocynate, and 2,4-dinitroaniline, the novel non-ionic surfactant 1-(2, 4-dinitrophenyl)-3-dodecanoylthiourea (DDT) was produced in high yield. Various spectroscopic techniques (^{1}HNMR, ^{13}CNMR, and UV-V) have been used to elucidate the chemical structure of DDT. Additionally, its electrochemical behaviour (electrochemical fate) was elucidated using a cyclic, square wave, and differential pulse voltammetry through a wide pH range. The limit of detection (LOD) and limit of quantification (LOQ) values of the compound were also determined using Square wave voltammetry (SWV). A fascinating fact observed is that the electroactive moieties in the compound are getting oxidized and reduced at a potential very close to 0.0 V, and the potential of the human body is 0.07 V, so the compound investigated can serve as an efficient candidate for the drug deliveries and metabolism processes.

1. Introduction

Surfactant compounds exhibiting an amphiphilic character contain hydrophilic (heads) and hydrophobic (tails) groups. They have a hydrophilic polar head with a long chain of hydrophobic hydrocarbons. In the previous, surfactant applications were limited to cleaning purposes, but recently, it has been a backbone of modern industrial uses. Surfactants, surface-active agents are among the most versatile products of the chemical industry employed in a variety of areas and recognized to play a vital role in many processes of interest in primary and applied science, such as paints, cosmetics, cleaners, pharmaceuticals, food, medicine, and biochemical research. Over the years the application of surfactants has increased significantly. Serval groups have investigated the application of surfactants in the field of electrochemistry (Nassar et al., 1997; Rusling and Nassar, 1993; Rajeshwar et al., 1994; Naveed et al., 2023; Rasheed et al., 2022). However, surfactants were first used in the electrochemistry by Hu et al., to increase the sensitivity of detecting different biomolecules. (Hu et al., 2007) The finding demonstrated a substantial enhancement in the electrochemical responses of these compounds when trace amounts of surfactants were introduced. They suggested a synergistic adsorption hypothesis to elucidate the mechanisms behind the surfactant-induced enhancements, for example, surfactants could potentially form specific interactions with the substrate, reinforcing their adsorption onto the electrode surface. (Hu et al., 2007;

Peer review under responsibility of King Saud University.
* Corresponding authors.
E-mail addresses: ahmadnaveed@ujs.edu.cn (A. Naveed), liguo@ujs.edu.cn (L. Guo).

https://doi.org/10.1016/j.arabjc.2023.105396
Received 23 August 2023; Accepted 26 October 2023
Available online 2 November 2023

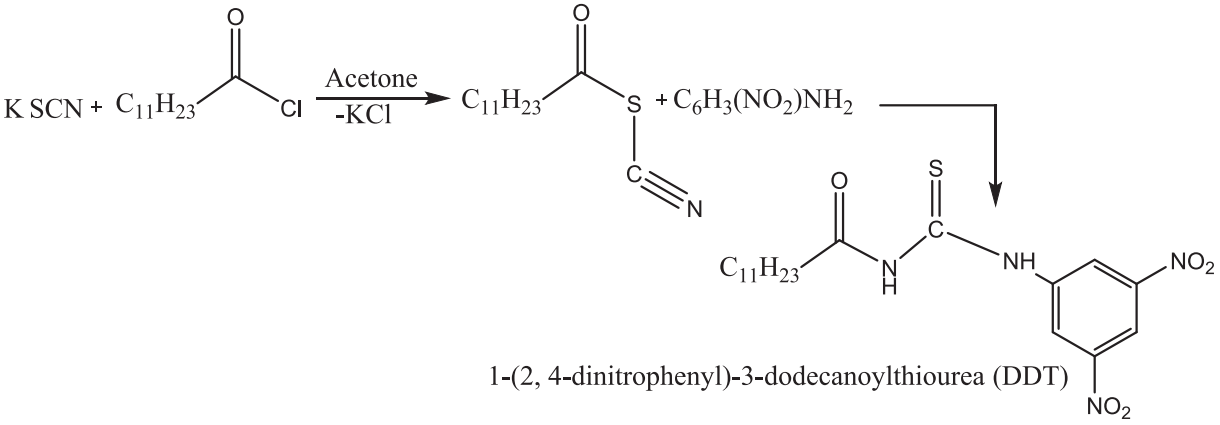

Scheme 1A. Synthetic scheme of 4-dinitrophenyl)-3-dodecanoylthiourea) (DDT).

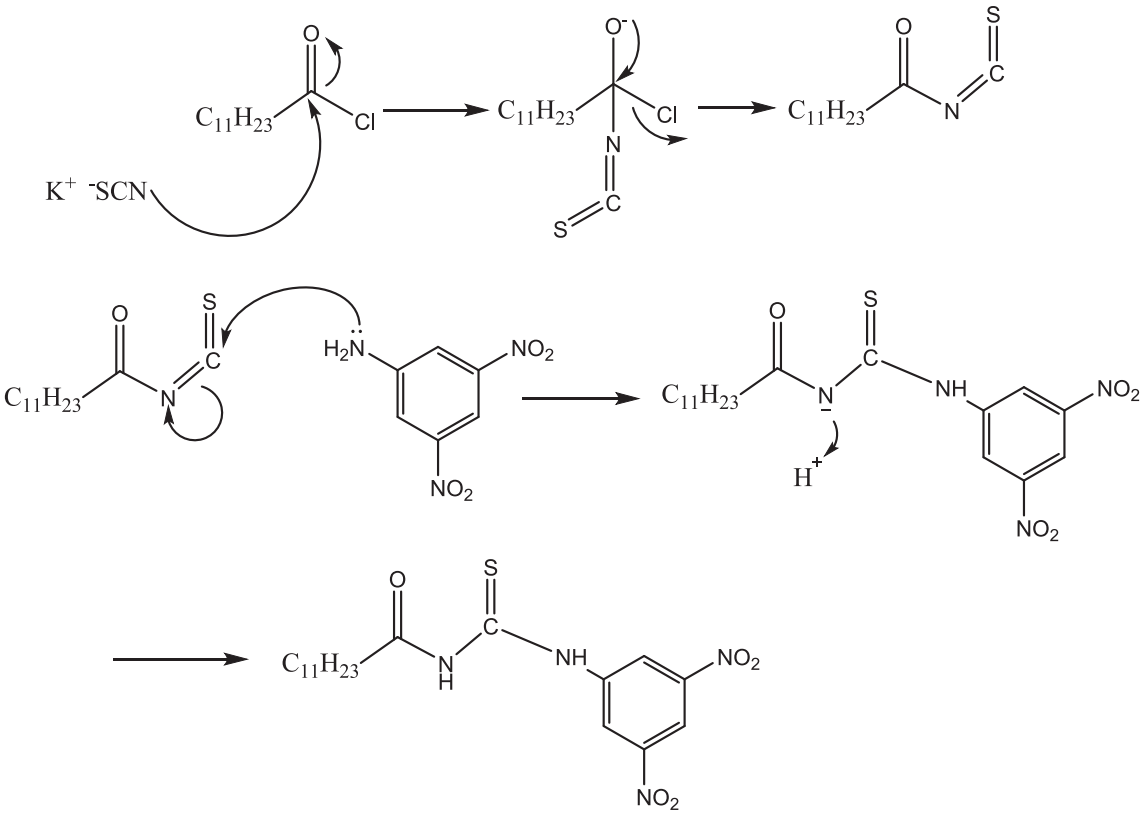

Scheme 1B. Proposed mechanism for 4-dinitrophenyl)-3-dodecanoylthiourea) (DDT).

Yi et al., 2001; Zhang et al., 2002; Hu et al., 2002) However, this interaction assisted the transformations of electrons among the electrodes and solution, resulting in modifications to the properties of the electrode/solution interface. Ultimately, these alterations influenced the electrochemical processes of the electroactive species. (Rusling and Nassar, 1993; Connors et al., 1985; Yang et al., 1999) (See Schemes 1A and Scheme 1B).

In this study, a new kind of nonionic surfactant based on thiourea has been developed and characterized.

According to the literature, nonionic surfactant serves efficiently in antibacterial activities. Many nonionic surfactants are thought to work at the membrane level but the specific role of nonionic surfactant based on thiourea remains unclear. (Ullah et al., 2014; Kubesch et al., 1987) However, the presence of single sulfur and two nitrogen atoms in the thiourea and their derivatives endows them with the potential to serve as corrosion inhibitors. (Kumar, n.d.; Wang et al., 2023; Qureshi et al., 2023) The presence of available electron pairs in the inhibitors facilitates the transfer of electrons to the metal surface from the inhibitor, resulting in the construction of a coordinated covalent bond. (Chauhan and Gunasekaran, 2007) The electrochemical examination of nitro-based compounds is an area of enormous interest. One factor contributing to this interest is that abundantly many nitro compounds are produced for the application of medications; as a result, they are significantly introduced into living things and frequently metabolized through redox-type reactions. In the literature, several authors have reviewed the electrochemistry of nitro compounds (Serrano et al., 2019; Squella et al., 2005) and made a reasonable conclusion that usually, phenomena of reduction are involved in consistent mechanism with a sequence of one-electron additions chemical steps; the variations are in the chemical follow-up reactions rather than the electrochemical stages.

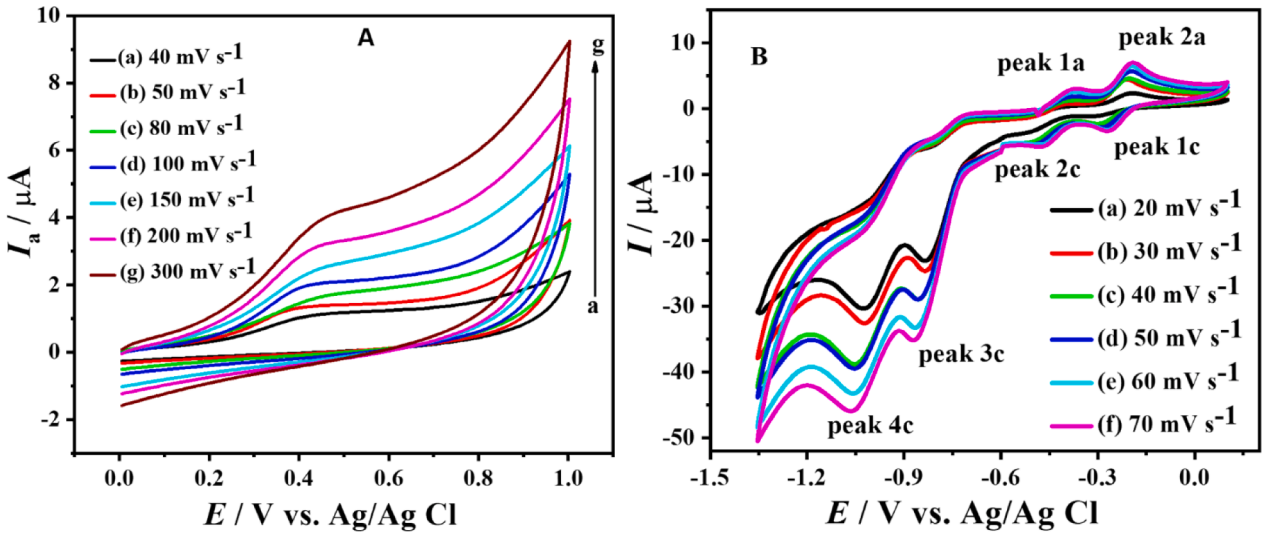

Fig. 1. CVs of 1 mM **DDT** in oxidation (A) and reduction (B) region at pH 10 and different scan rates.

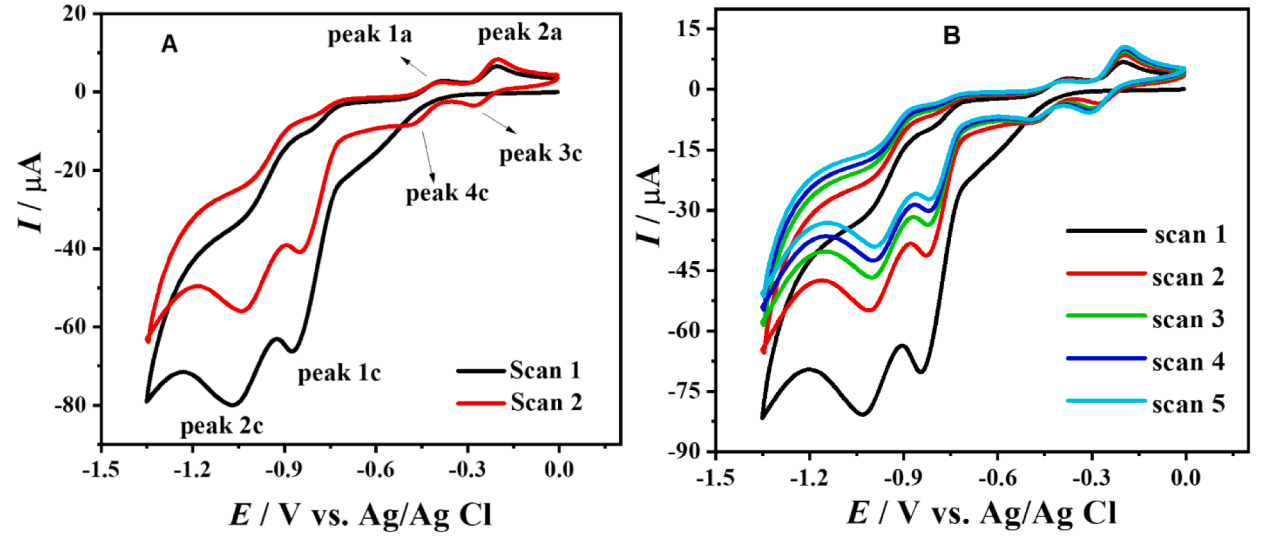

Fig. 2. CVs of 1 mM **DDT** at pH 10 showing first and second scan (A) and multiple scans (B) at 100 mV $s^{-1.}$

Over the last two decades, organic electrochemists extensively researched the electrochemical reduction mechanisms of heterocyclic nitro and aromatic compounds. These investigations showed that the processes are highly complicated and are greatly influenced by the characteristics of the reaction medium.

Although extensive literature is available on the electrochemistry of nitro compounds, the electrochemical fate of thio urea-based surfactants containing nitro groups is unexplored. (Ullah et al., 2014; Wu et al., 2020; Bhattacharya and Bajaj, 2009) The incorporation of thio group and nitro groups in the compound examined has made it an incredibly motivating probe for electrochemical investigation. It is expected that detailed electrochemical probing of this compound will open up new routes in the mechanistic pathways of nitro compounds which are not being delved in to research arena.

2. Experiments

2.1. Materials and method

Lauryl chloride (Sigma Aldrich,98 %), Potassium thiocyanate (KSCN) (Sigma Aldrich,99 %), and different derivatives (primary and secondary) of aliphatic and aromatic amines can be used; for example, 2,4-dinitroaniline and 2-chloroaniline (Sigma Aldrich 98 %) and Bromo ethane (Sigma Aldrich 98 %) were used for synthesis. Fresh dry acetone (free from any water or moisture) was used as a solvent, and analytical-grade acetone was dried before the experiment in the laboratory. During the experiment, products were confirmed using thin-layer chromatography (TLC). For structure elucidation, ^{1}HNMRspectras were recorded using Bruker AC Spectrometers at 300.13 MHz. For UV–Visible analysis, the UV-1601Shimadzu spectrophotometer has been used. In contrast, electronic absorption was recorded on a UV-1800 Shimadzu spectrometer. By using WTW Lab pH 720 m, pH was analyzed. The Digi-Ivy DY2113 Potentiostat, USA was used for Voltammetric analysis. Analyte working solution exhibiting 50 % water and ethanol and supporting electrolytes. Differential pulse voltammetry (DPV) was performed with a scan rate of 5 mV s-1. For square wave voltammetry (SWV), the working condition was adjusted at 20 Hz, and 5 mV potential increases to regulate a scan rate of 100 mV s-1. All desired voltammetric experiments were performed at room temperature under a nitrogen atmosphere.

In addition, the glassy carbon electrode (GCE) was significantly applied as a working electrode, Pt-based wire assisted as a counter electrode, and Ag/AgCl was used as a reference electrode. According to

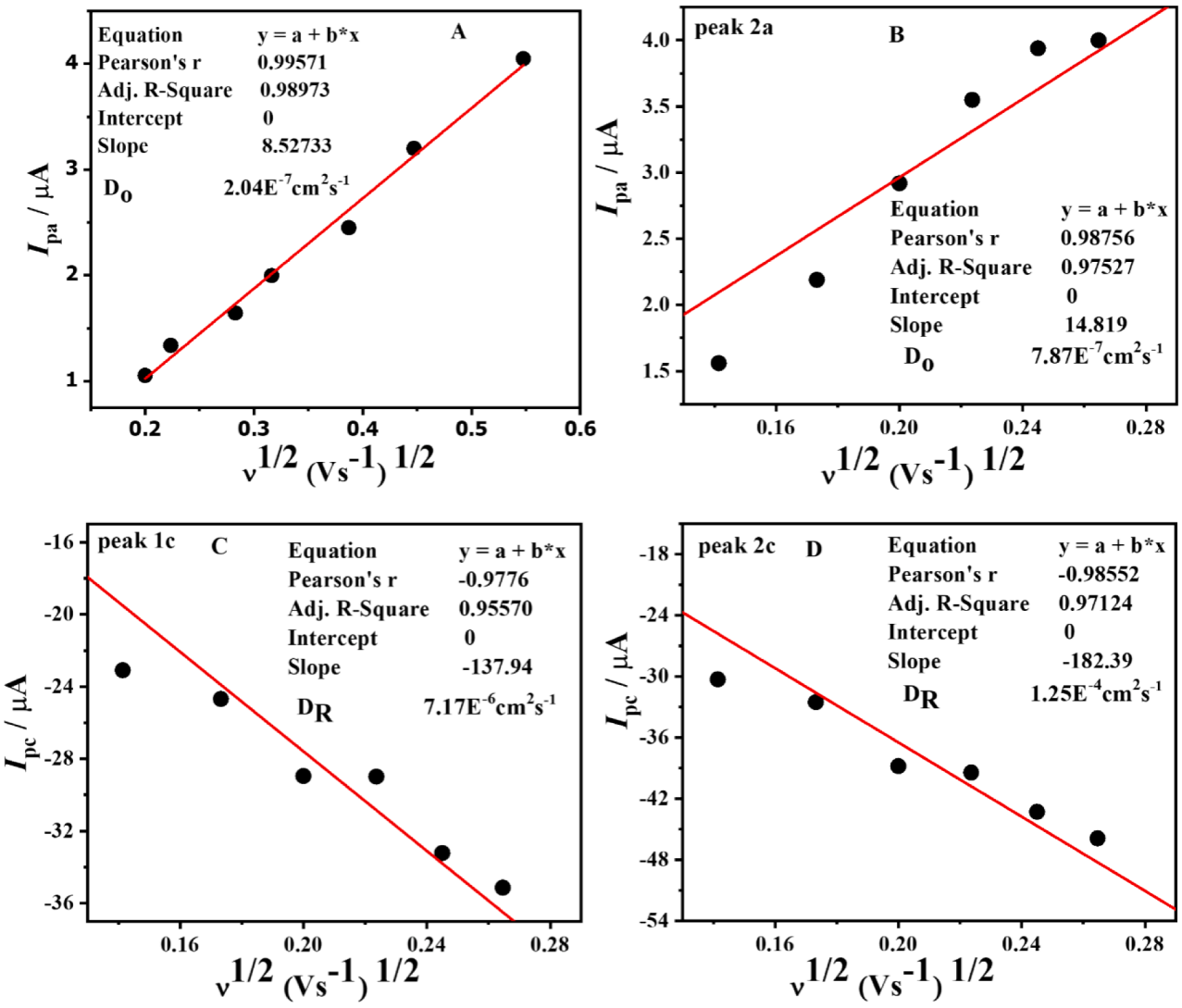

Fig. 3. Plots of anodic (A and B) and cathodic (C and D) peak currents of **DDT** vs square root of scan rate at pH 10.

the literature, several studies exhibited the active area GCE with a charge of 0.063 cm2. However, before the experiments, the working electrode surface was required to be polished with alumina powder and washed with distilled water.

2.2. Synthesis

2.2.1. Synthesis of 4-dinitrophenyl)-3-dodecanoylthiourea) (DDT)

To synthesize DDT, 0.6 g (0.0063 mol) of potassium thiocyanate was dissolved in 50 mL of dry acetone, adding 1.5 mL (1.30 g) of lauryl chloride and stirring the mixture for 60 min. Next, 2, 4-dinitroanaline was added, and the solution was kept on stirring for another 12 h. However, the achieved product was significantly washed using distilled water to remove the impurities; the yield was 78 %, with yellow color and soluble in hot water and ethanol. The purity and structure of the compound were determined by NMR spectroscopy and spectral details in the below.

^{1}H NMR (300 MHz, CDCl3, δ-ppm): 12.56 (1H, s, ^{2}NH), 11.07 (^{1}H, s, ^{1}NH), 8.75 (2H,d, 2CH, ^{3}J [^{1}H, ^{1}H] = 15 Hz), 7.78 (^{1}H,s, CH), 2.46 (2H, t, $^{8}CH_2$, ^{3}J [^{1}H, ^{1}H] = 15 Hz), 1.38–1.29 (18H, m, 9CH_2), 0.90 (3H, t, CH_3, ^{3}J[^{1}H–^{1}H] = 12 Hz).

^{13}C NMR (75.5 MHz CDCl3, δ-ppm): 180.0 (C_6), 174.5 (C_7), 134.1 (C_5), 133.3 (C_4), 128.9 (C_1), 126.7 (C_3), 123.9 ($C_{2,2}$), 37.8 ($C_{8,}$), 22.6–31.8 ($C_{9\text{-}17}$), 14.9(C_{18}).

3. Result and discussions

3.1. Cyclic voltammetry of DDT

Using the potential range between (0 → 1.0 V) and the scan rate of 100 mV s-1, a Cyclic voltammogram of 1 mM DDT was initially recorded. A supporting electrolyte with a pH of 10.0 was used to enhance the visibility of the signals. The signals obtained at this pH medium were found to be more pronounced and distinct. At a scan rate of 100 mV s-1, an irreversible anodic peak at + 0.416 V matching to the compound's oxidation was seen. With an improved scan rate, the anodic peak moves to greater positive potentials (Fig. 1**.A**).

In order to examine the reduction of the compound, a cyclic voltammogram was recorded in the potential range of 0 → -1.35 V at a scan rate of 100 mV s^{-1} using a supporting electrolyte of pH 10.0, as shown in Fig. 2**.B**. In the first scan, two reduction peaks (peak 1c and 2c) at −0.743 V and −0.934 V were observed and significantly represented the reduction of the compound in the foreword scan, and two oxidation peaks (peak 1a and 2a) at −0.393 V and −0.203 V respectively were witnessed in the backward scan due to the oxidation of the reduced products of the compound. Now in the second scan, along with peaks 1c and 2c, two new cathodic peaks were labelled as 3c and 4c, corresponding to the reduction of the oxidized product of signal 1a and 2a, respectively, which were absent in the first scan. The performance of our

Table 1
Diffusion Coefficients of **DDT.**

Peaks	Anodic peak (D_o)	Peak 2a (D_o)	Peak 1c (D_R)	Peak 2c (D_R)	Peak 3c (D_R)
Diffusion coefficient (cm^2s^{-1})	2.04×10^{-7}	7.87×10^{-7}	7.17×10^{-6}	1.25×10^{-4}	2.29×10^{-7}

synthesized non-ionic surfactant is significantly influenced by the stability of cyclability, which encompasses the ability to maintain a high reversible capacity even at high scan rates. As noted, an irreversible anodic peak at a potential of + 0.416 V, which corresponds to the oxidation of the compound, was seen when the scan rate was set at 100 mV s-1. The peak voltage has significant importance since it serves as a crucial metric, signifying the potential at which the oxidation process takes place. The relationship between the peak current density and the scan rate is direct, indicating the rate of oxidation. The peak efficiency, defined as the ratio of the peak current density to the scan rate, provides valuable information on the efficiency of the oxidation process.

The electronic effects in DDT can be discussed in the context of the spin-polarization mechanism. Spin polarization refers to the phenomenon where the spin of an electron influences its energy levels, leading to different chemical behaviors. This mechanism could potentially explain the observed electrochemical behavior of DDT, including its electrochromic properties, hydrogen oxidation, and water splitting. Moreover, the compound possessing different functional moieties is indicative that the compound can be utilized in multi-disciplinary application areas like water splitting and hydrogen production etc.

However, recording multiple CV scans (Fig. 2.**B**) without washing the electrode surface revealed that the two significant cathodic signals that are peak 1c and 2c, were moved to more positive potential values accompanied by a decrease in peak intensity which shows the adsorption of analyte on the electrode surface. As mentioned that in the latter scans peak current of the indicated cathodic signals decreases at the same time the peak intensity of the anodic signals 1a and 2a along with their respective cathodic signals increases, which shows that peaks 1a and 2a are observed due to the reduced product of 1c or 2c. Cyclic voltammograms of the compound were recorded in the reduction region at different scan rates, as shown in Fig. 1**. B** The perceptive identification of the irreversibility of the cathodic signals in the initial scan is noteworthy. It is probable that the chemical is undergoing a further reaction, wherein it acquires three protons and releases water molecules, resulting in the formation of the reduced product of the compound.

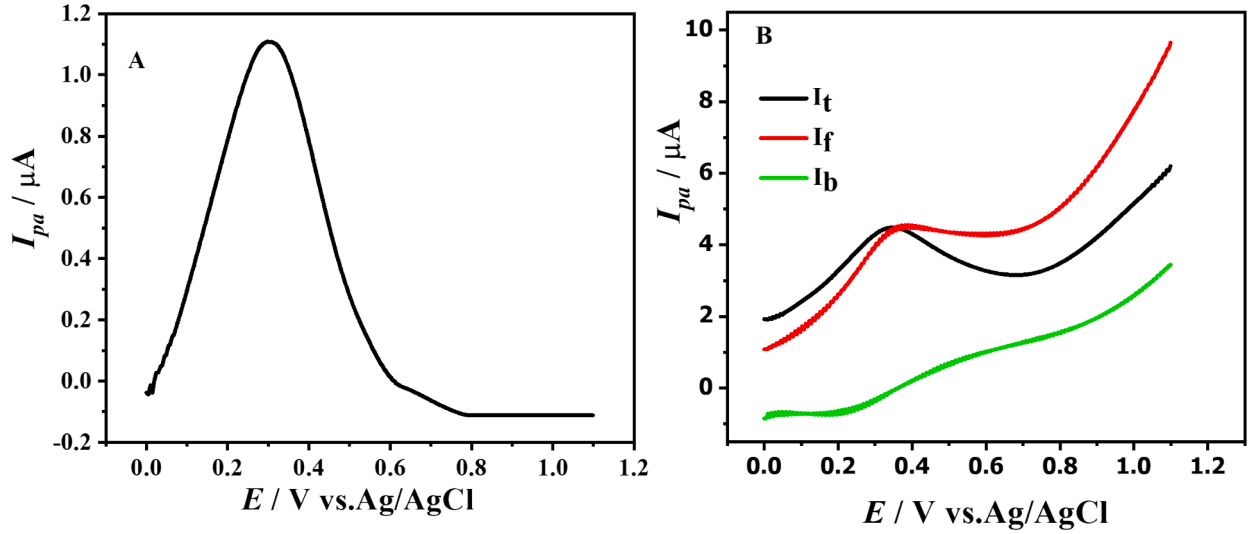

Fig. 4. SW voltammogram showing the oxidation of **DDT** at pH 7 (A) and along with forward and backward current components (B) at 100 mV s^{-1}.

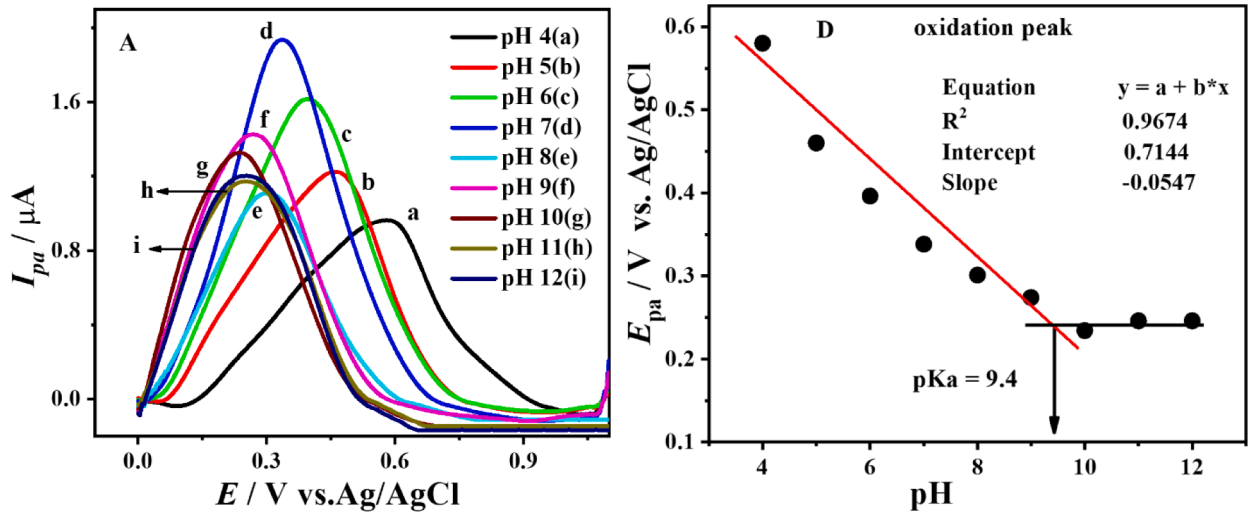

Fig. 5. SW voltammogram displaying oxidation of **DDT** at pH 4–12 (A) and plot of E_{pa} vs pH (B) at 100 mV s^{-1}.

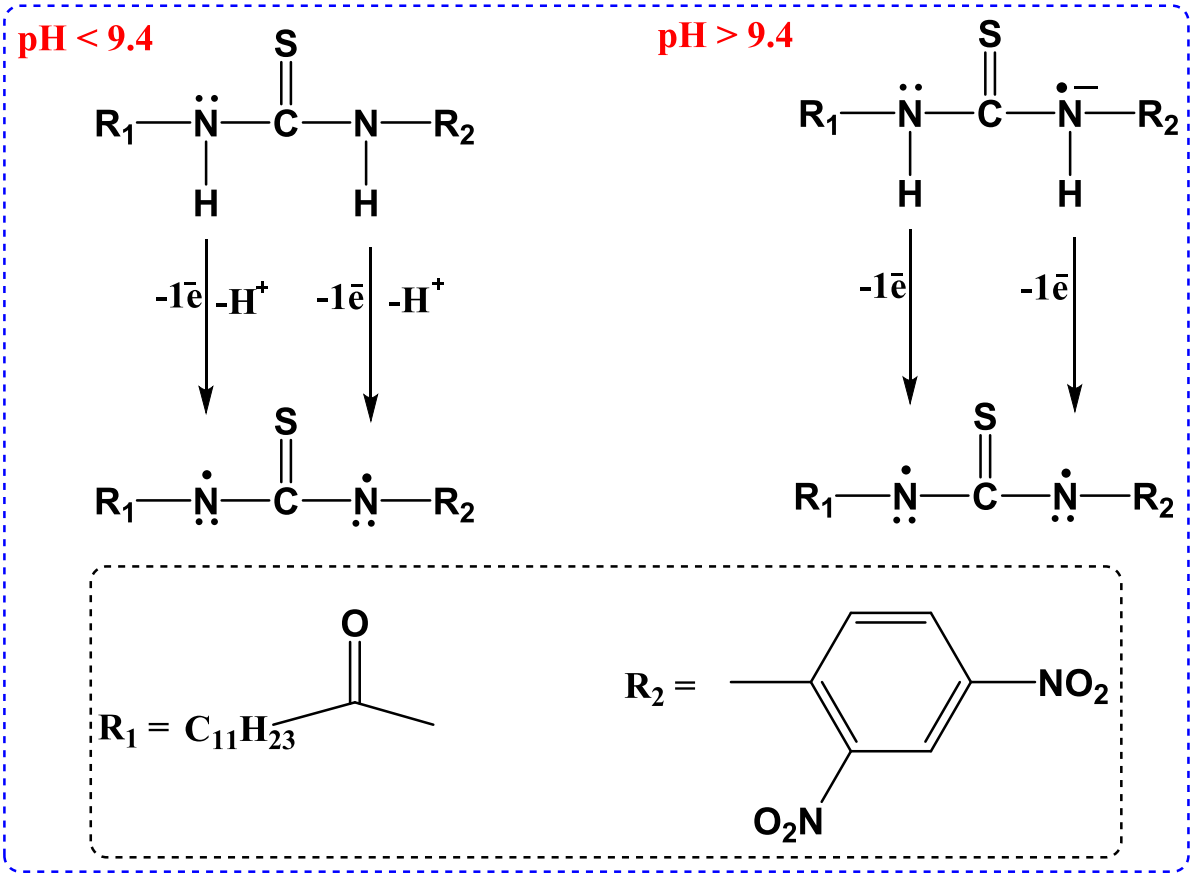

Scheme 2A. Electro-oxidation mechanism of **DDT.**

Nevertheless, it is imperative to acknowledge that the aforementioned statement is a preliminary hypothesis.

By visualizing the anodic and cathodic currents vs. the square root of the scan rate, we could use the Randles Sevcik equation to get the diffusion coefficients for oxidation (D_o) and reduction (D_R) of the compound. (Melese et al., 2023) Fig. 3 **A, B, C, D** for anodic signal, peak 2a, peak1c, and peak2c, respectively. The values of the diffusion coefficients calculated are listed in the Table 1.

3.2. Square wave voltammetry (SWV) of DDT

(a) Electro-oxidation of compound

In order to examine the behaviour of the oxidation signal of the compound in different pH media, SWVs of the compound were obtained in a wide pH range. It was discovered that the peak potentials of the wide oxidation signal are very sensitive to the medium of the pH. As seen in cyclic voltammograms of the compound in the potential range of 0 → 1.0 V, there is a single broad peak observed, which corresponds to the electro-oxidation of the compound. In SWVs also, a single broad pH-dependent irreversible peak is noticed at + 0.302 V, SWV showing electro-oxidation of the compound in a medium of pH 7 is shown in Fig. 4**.A**. SWVs, obtained in the pH range 4–12, discovering the shifting of the anodic peaks to lower positive potential values with an increase in pH of the medium up to pH 10, and under highly alkaline conditions of at pH 11 and 12 there is no change in peak potentials. The acetone acquires a prominent role in this process. It is crucial to acknowledge that acetone demonstrates a discernible behavior when engaging with other solvents inside the matrix. This kind of behaviour from actone can be attributed to its polarity and moleculer structure, which allow its to interact with various solvents Consequently, these interactions have an impact on the electro-oxidation process of the compond. In addition, The pH of the electrolyte is also a crucial factor in the electro-oxidation process. Changes in pH can impact the electrochemical potential and hence affect the viability of a redox reaction, ultimately influencing the oxidation state of the substance. The compound's electrocatalytic activity and stability may be subsequently influenced by this.

From the intersection point of the two trends in E_{pa} vs. pH plot Fig. 5**. B**, the pka of the compound was evaluated as 9.4. So it was inferred that the compound is present in the protonated form up to pH 9.4, and after that it gets deprotonated. The dependence of peak potentials on pH shows that electro-oxidation of the compound involves the transfer of electrons and protons. The slope value of E_{pa} vs. pH plot indicated that oxidation phenomena significantly required equal protons and electrons.

The SWVs of the anodic signal recorded in the pH range 4–12 are shown in Fig. 5**.A.** To inspect the nature of oxidation, peak forward and backward current components of SWV were plotted along with total current, recorded in a 1 mM solution of compound buffered at pH 7 as shown in Fig. 4**.B**, which testifies the irreversible nature of the oxidation signal.

(b) Proposed oxidation mechanism of DDT

The electro-oxidation mechanism of **DDT** has been proposed based on the results of all three electrochemical methods (See Scheme 2A). Below pH 9.4, both the nitrogen atoms oxidize by the loss of one electron and as well as one proton to form the mentioned product; above pH 9.4, the compound is present in deprotonated form, hence the electro-oxidation process is undergone by the loss of electrons only and there is no involvement of protons. The electron pair on both the nitrogen atoms is extensively involved in delocalization with R_1 and R_2 along

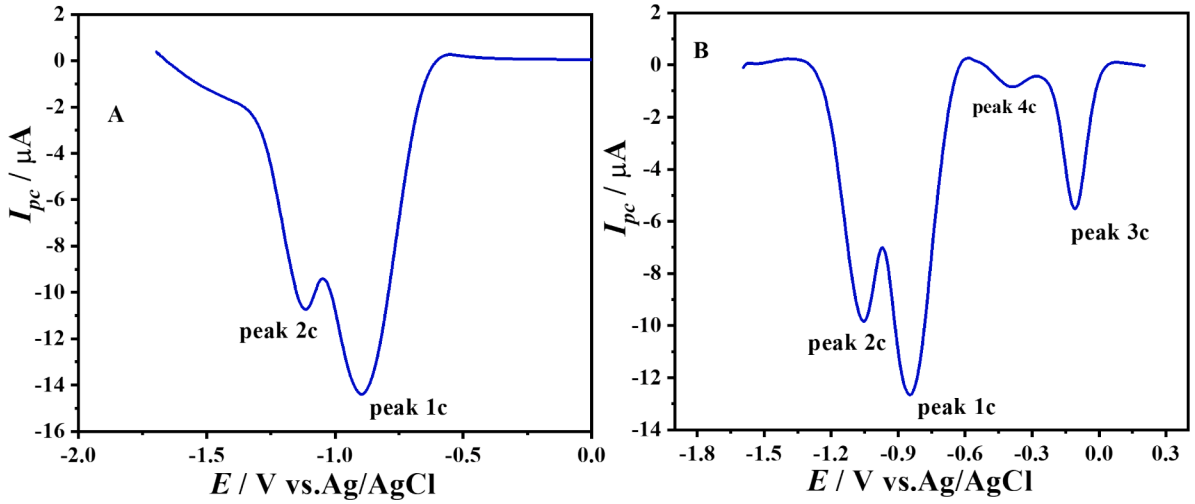

Fig. 6. SW voltammograms showing reduction of **DDT** scan 1 & scan 2 at pH 7.

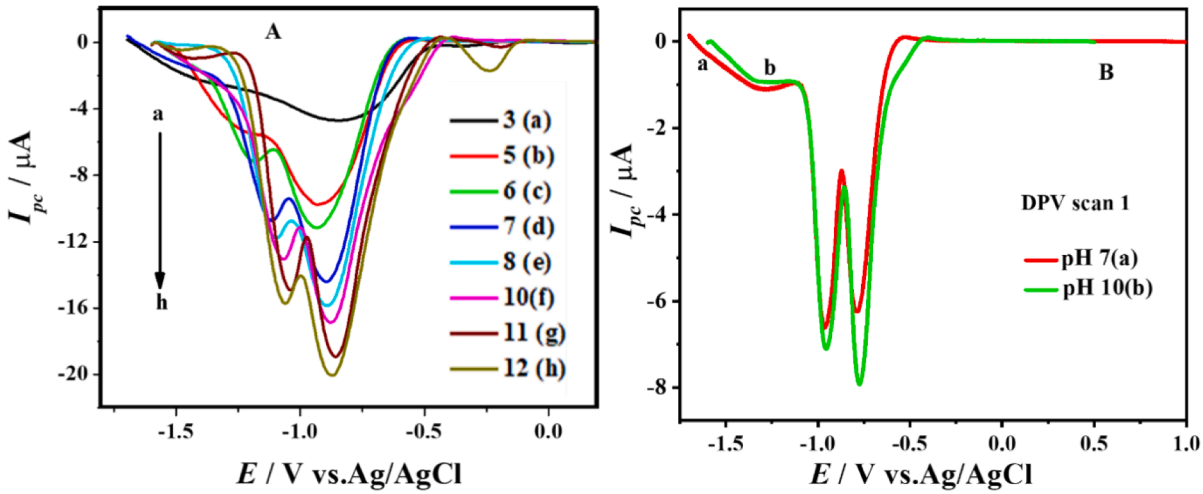

Fig. 7. SW and DP voltammograms of **DDT** in reduction region at different pH media.

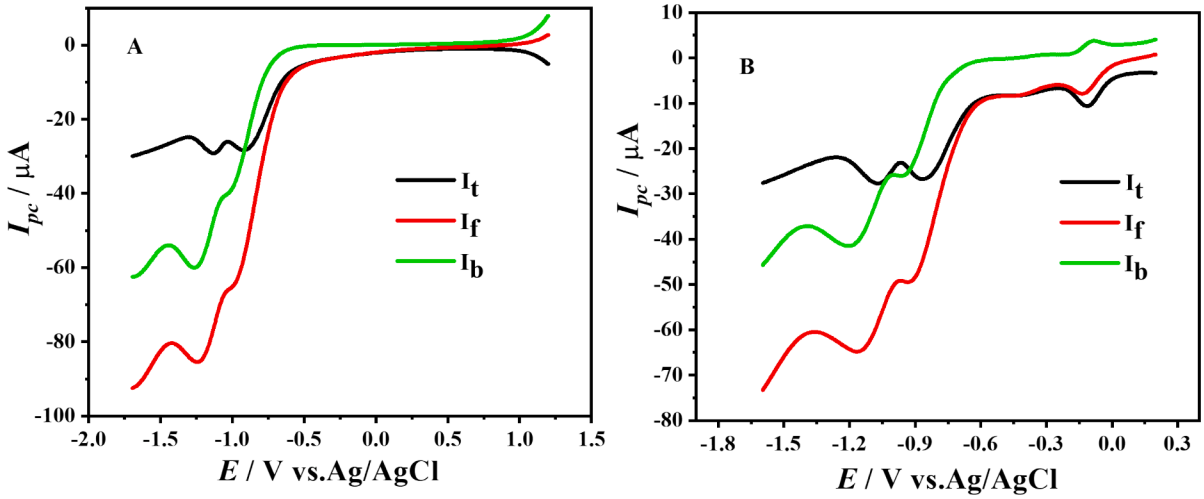

Fig. 8. SW voltammograms scan I (A) and scan II (B) of 1 mM **DDT** at pH 7 showing total current (I_t), forward current (I_f) and backward current (I_b) at 100 mV s^{-1}.

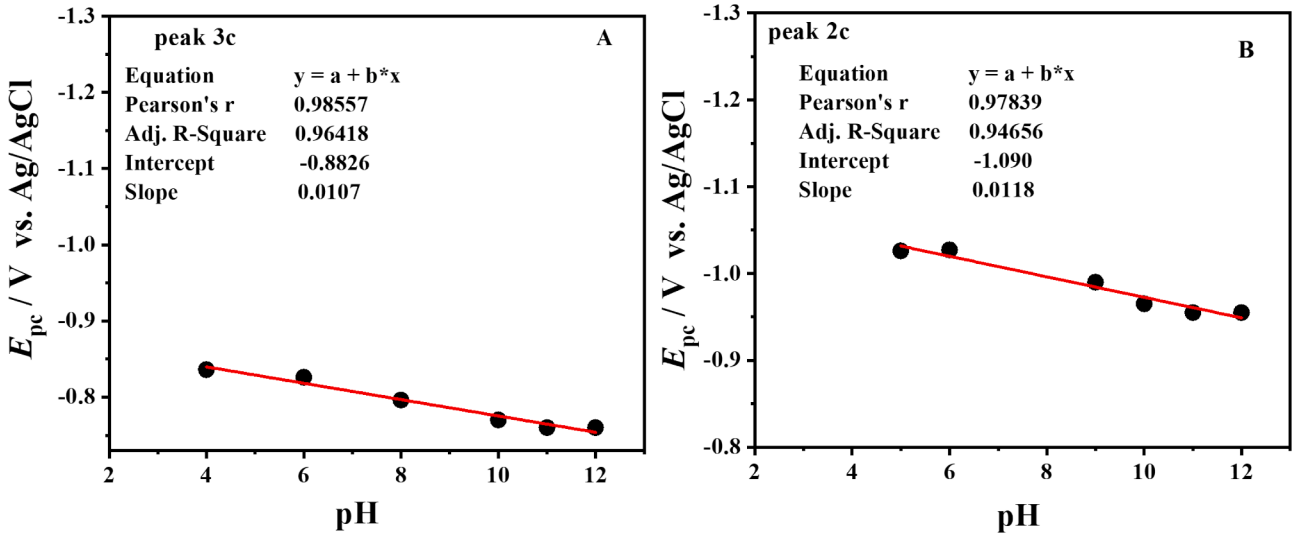

Fig. 9. Plot of E_{pc} vs. pH peak 1c (A) and peak 2c (B) of **DDT.**

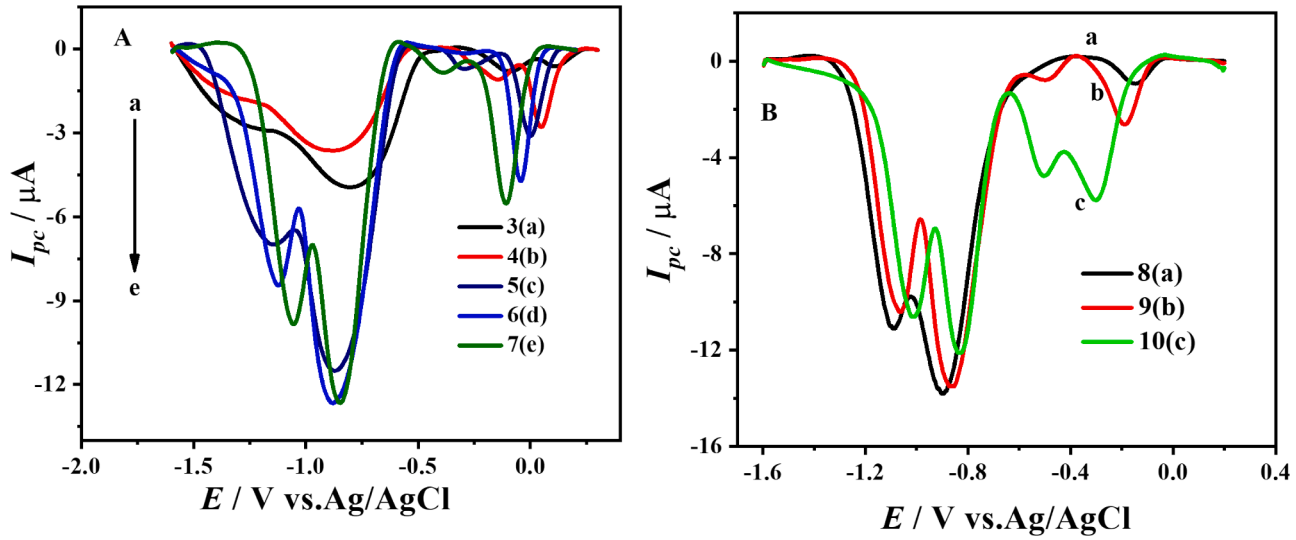

Fig. 10. SW voltammograms of **DDT** in reduction region at different pH media.

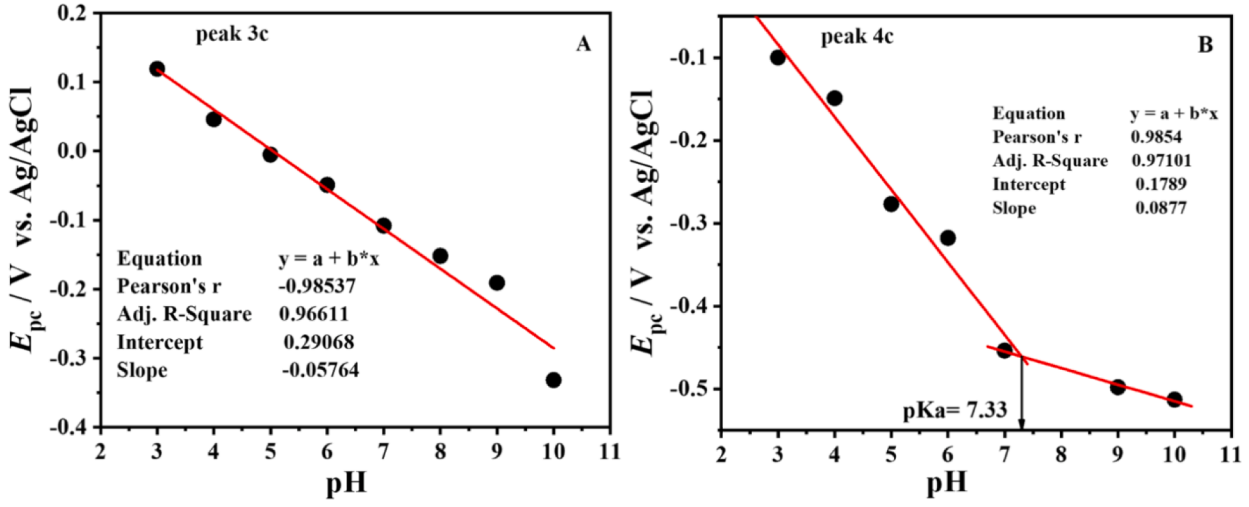

Fig. 11. Plot of E_{pa} vs. pH for peak 3c (A) and peak 4c (B) of **DDT.**

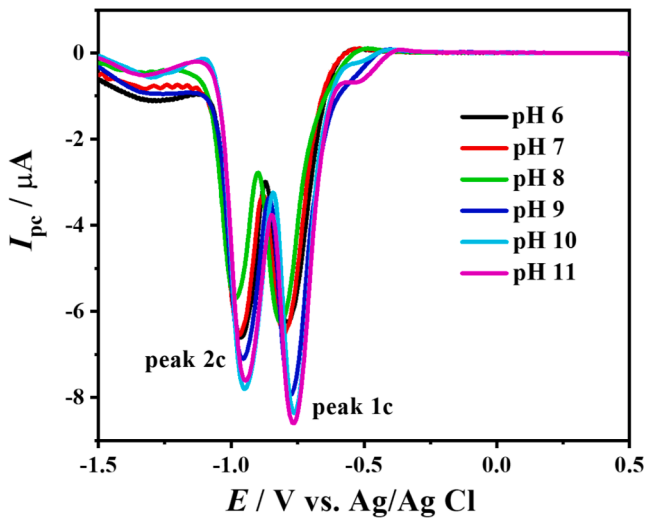

Fig. 12. DP voltammograms of 1 mM **DDT** in different pH media.

with thio group; the lone pair on the nitrogen atom linked with R_2 is somewhat more intensely delocalized due to the presence of nitro groups on the benzene ring hence both the nitrogen atoms are not present in the same environment which is making the nitrogen atoms not to oxidize precisely at the same potential but in a very close potential range resulting in the formation of a broad peak.

(c) Electro-Reduction of compound

In the case of electro-reduction of the compound, during the first scan, as shown in Fig. 6.**A** two irreversible peaks, which were labelled as 1c and 2c, appeared at –0.898 V and −1.115 V respectively in SW voltammogram at 100 mV s^{-1} in a medium of pH = 7. During the second scan under the same conditions, two new peaks came into sight labelled as 3c and 4c at −0.109 V and −0.393 V, respectively, as shown in Fig. 6. **B** which was due to the reduced product of the compound in the first scan. The same signature was also witnessed in the second cyclic voltammetric scan. So the SW voltammetric results are complementing the CV results.

To propose redox mechanism for the electro reduction of the compound, SWVs were recorded in the pH range of 3–12 both for the first and second scans. Fig. 7 shows the first scans of SWVs for the electro reduction of the compound in the pH range 3–12. A single broad peak was observed at pH 3, this broad peak starts splitting in to two distinct peaks as the pH of the medium increases to more alkalinity accompanied with an increase in current intensity as well as shifting of peak potentials to more positive values. This signal is indicative of the presence of protons throughout the reduction process and the relative simplicity of the reduction in more fundamental media. Differential pulse voltammograms were taken in a 7 and 10 pH medium to investigate the number of electrons involved in the reduction of the chemical (Fig. 7.**B**). The peak width of 91 mV for both the reduction peaks in the first scan evidenced one electron transfer in each case. Plotting the forward and backward current components of SWV alongside the total current allowed us to investigate the reversibility of cathodic peaks. The voltammograms presented in Fig. 8. **A** and **B** evidenced the irreversible nature of both cathodic peaks in the first scan and the reversible nature of peaks 3c and 4c in the second scan, respectively. Peak potentials of both reduction peaks considering the first scan were plotted against pH and are shown in Fig. 9.**A** and **B**.

To investigate the effect of pH on the cathodic peaks appearing in the second scan, SWVs of the second scan were recorded in the pH range 3–10. The behaviour of cathodic peaks **1c** and **2c,** which were also present in the first scan, is more or less the same as discussed in the case of scan 1, but the new cathodic peaks arising in the second scan, named as **3c** and **4c** shifts to more negative potential values as the pH of medium increases accompanied with an increase in peak intensity as shown

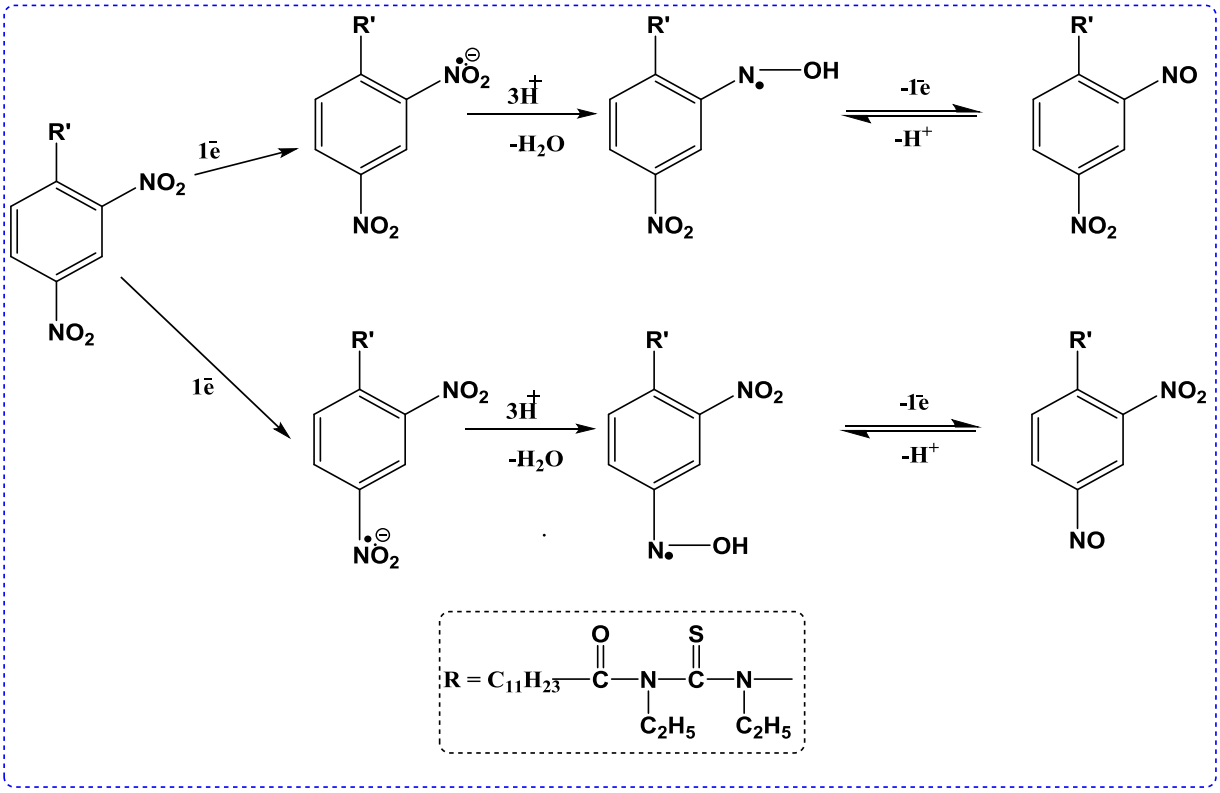

Scheme 2B. Electro reduction mechanism of **DDT.**

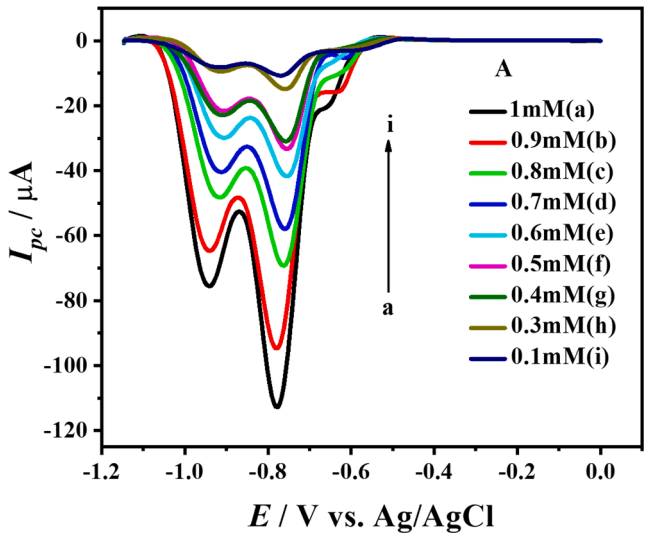

Fig. 13. SW voltammograms of **DDT** at different concentrations.

in Fig. 10**. A and B**. Another interesting fact is that these electroactive moieties are getting reduced at a potential very close to 0.0 V, and the human body potential is 0.07 V, so the compound under investigation can serve as an efficient probe for drug delivery. However, the redox potential is a measure of the tendency of a chemical compound to undergo oxidation (loss of electrons) or reduction (gain of electrons).

Peak potentials of the two new reduction peaks evidenced in the second scan are plotted against pH and are portrayed in Fig. 11**. A** and **B**.

To investigate the medium effect on the reduction signals, differential pulse voltammograms were also recorded in different pH media Fig. 12 and the same pH-independent nature of peaks 1c and 2c was observed, as portrayed in Fig. 7.

(d) Proposed reduction mechanism of DDT

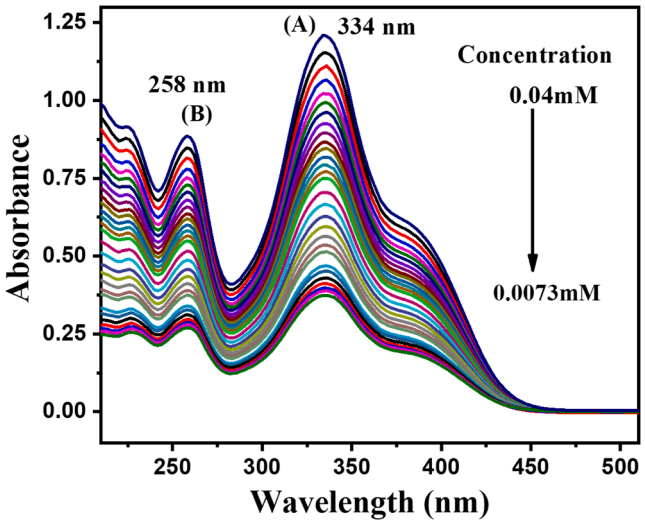

Fig. 15. UV–visible spectra of **DDT** at different concentrations.

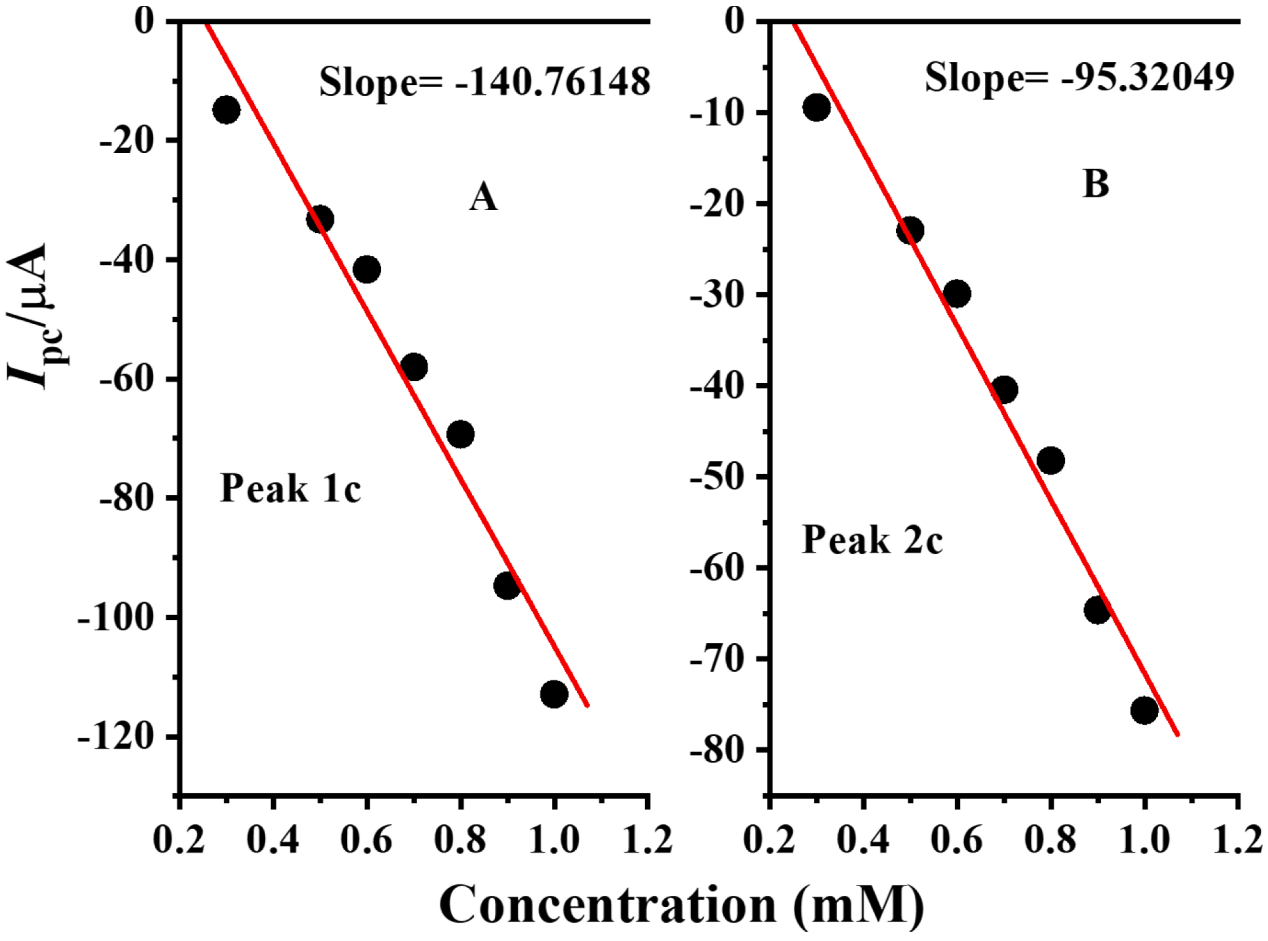

Fig. 14. Plots of cathodic peak currents of **DDT** vs concentration.

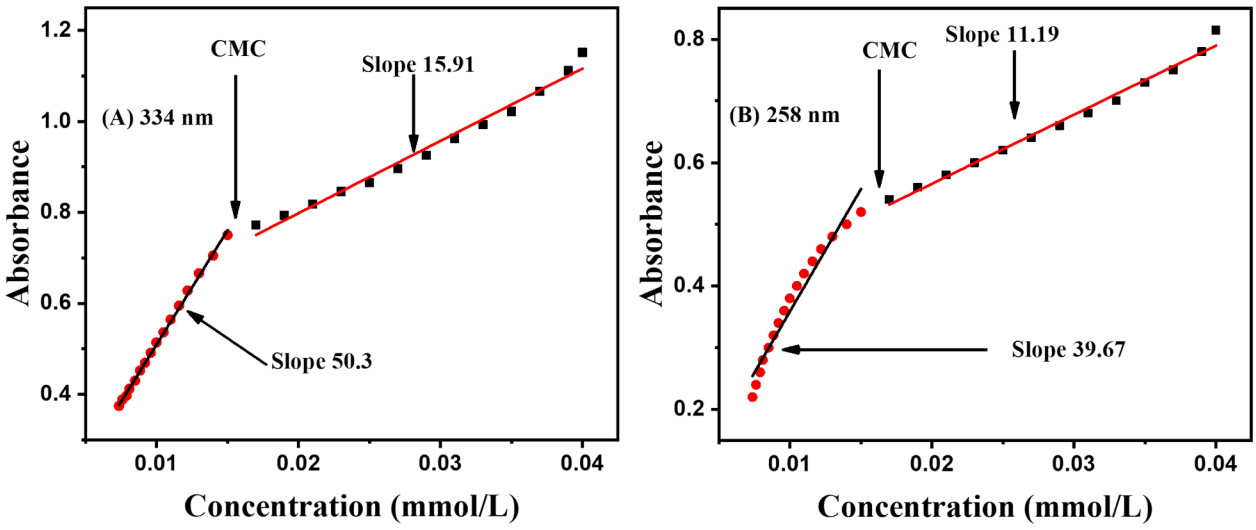

Fig. 16. Plot of absorbance vs concentration of **DDT** at 334 nm and at 258 nm.

In general, the reduction of nitro-groups involves in the methemoglobinemia and gastro-intestinal microflora inducement, leads to amines in complexes that exhibiting the electron-withdrawing groups. It provide a clear indication for the one-electron transfer mechanism in the reduction process. On the other hand, the EC2 mechanism which involved in the electrochemical reactions of organic molecules is crucial, particularly in proton-coupled electron transfer reactions. The literature suggests that this mechanism includes the nitro group undergoing a six-electron transition as a result of the addition of two protons and three electrons.

However, in the reduction mechanism of DDT, both the nitro groups got reduced by the gain of one electron each as there is no experimental evidence of the involvement of protons in the reduction of the compound considering the first scan (See Scheme 2B). Due to the irreversible nature of both the cathodic signals in the first scan, we can suggest that the compound is undergoing a follow-up reaction by gaining three protons each and losing water molecules to form the reduced product of the compound. Now because we are getting two reversible pH-dependent redox couples in the second scan, it is proposed that the reduced product of the compound is oxidizing in a reversible fashion by losing one electron and one proton each to form the nitroso product. Overall, the nitro group has been converted to nitroso group. In the kinetics of reversible deprotonation, the proton is transferred from the compound to the base, and the concentration factor can influence it. Additionally, the kinetics of the reversible deprotonation of 1-(2, 4-dinitrophenyl)-3-dodecanoylthiourea types compounds, particular focus on the redox-dependent H-bonding and the impact of one electron versus two-electron redox couples. Generally, organic solvents, such as dimethyl sulfoxide, acetonitrile and dichloromethane, can be used as electrolytic media. In addition, these solvents are less likely to quench the radical reaction and facilitate the generation of radicals during the electrolyte process.

To determine the heterogeneous electron transfer rate constant, SWVs of the compound using solutions of different concentrations of the compound buffered in a medium of pH 10 were recorded considering the first scan and are shown in Fig. 13.

By plotting the peak currents of cathodic peaks vs. concentration as portrayed in Fig. 14 and hence using the slope values in the Reinmuth equation, heterogeneous electron transfer rate constants were determined for both peaks. The values of heterogeneous rate constant for peaks 1c and 2c are 2.31×10^{-5} cm s^{-1} and 1.56×10^{-5} cm s^{-1}, respectively.

LOD and **LOQ** values were also evaluated for the compound having values of **0.100 mM** and **0.3364 mM** respectively.

3.3. UV–visible spectroscopy of DDT

It is well known that the thiourea-based compounds exhibit low solubility in eques solution mainly due to thiourea moiety but show good solubility in polar and non-polar organic solvents such as toluene. Over the last two decades, several thiourea-based surfactants have been investigated with their Critical Micelle Concentration (CMC) in organic solvents. For thiourea-based surfactants, such as 1-(decanoyl)-3-(4-ferrocenylphenyl) thiourea (DP) showed a strong peak of 259 nm and 280 nm in ethanol. (Ullah et al., 2014).

UV–Visible spectra of DDT were recorded at different concentrations, as portrayed in Fig. 15, using ethanol as a solvent, which captured two signals one at the lower wavelength (258 nm) is labelled as **B** and the one appearing at a relatively longer wavelength (334 nm) is marked as **A**. The compound was characterized by the wavelength of maximum absorbance and molar absorptivity coefficient values. The values are $\lambda_{max} = 334$ nm, $\varepsilon = 2.51 \times 10^4$ $M^{-1}cm^{-1}$. As illustrated in Fig. 16, the Critical Micelle Concentration (CMC) can be calculated by plotting the absorbance against concentration. However, in this method, utilized the intersection of the tangents to the x-axis to determine the CMC. By sketch a perpendicular line from this intersection point, leading to identify the CMC precisely. According to the literature, this method has been broadly used in the field of surfactant research and provided reliable results. (Fuchs-Godec, 2006; Bayol et al., 2008).

In our approach, we utilized the intersection of the tangents to the x-axis to determine the CMC. By drawing a perpendicular line from this intersection point, we could identify the CMC value accurately. This method has been widely used and accepted in surfactant research and has provided reliable results in previous studies. According to the investigation of Imdad Ullah et al., non-ionic thiourea-based surfactants obtained at room temperature, the critical micelle concentration can be determined by plotting absorbance versus concentration. The plots presented two linear parts with different slopes, and the critical micelle concentration was evaluated from their intersection. The significant variation in the hydrophobic fragment led to an alteration in the CMC. However, decreased carbons' chain length led to increases in CMC values of thiourea-based non-ionic surfactants. (Ullah et al., 2014).

This process can also be explained by implementing the Lambert-Beer Law through the relationship between absorbance (A) and concentration (c) for the DDT at the wavelength of 334 nm. The Lambert-Beer Law is expressed in equation 1. $A = \varepsilon * c * l$, whereas A is the absorbance, ε is the molar absorptivity coefficient, c is the concentration, and l is the path length. To calculate the CMC (Critical Micelle Concentration), the plot of absorbance against concentration in Fig. 16,

typically at the wavelength of maximum absorbance (λmax), which is 334 nm. CMC) is a concentration at which surfactant molecules start to aggregate to form micelles. This process can significantly affect the absorbance, as it changes the local environment of the compound. Typically, below the CMC, the absorbance might follow the Lambert-Beer Law, but beyond the CMC, the presence of micelles can cause deviations in the absorbance-concentration relationship. The CMC is an essential parameter when studying the behavior of surfactants or amphiphilic compounds in solution, as it marks the point where self-assembly into micelles occurs.

4. Conclusion

A novel non-ionic surfactant 1-(2, 4-dinitrophenyl)-3-dodecanoylthiourea (DDT) was synthesized with high yield by the reaction of the appropriate amount of lauryl chloride, potassium thiocynate and 2,4-dinitroaniline. The spectroscopic techniques ^{1}HNMR, ^{13}CNMR, and UV-V were used for the structure elucidation, respectively. The under-consideration compound was found to oxidize and reduce at the surface of the glassy carbon electrode. In addition, cyclic, square wave and differential pulse voltammetry have been use to investigate the electrochemical fate of the compound in a wide pH range. Based on results obtained from three electrochemical techniques, redox mechanisms of the compound were proposed. Electron abstraction and capture occurred in a pH-dependent manner. Parameters like pKa, LOD, LOQ, ksh, and D were successfully determined from voltammetric data. The redox behaviour of DDT followed an irreversible pH-dependent oxidation process controlled through partial diffusion and partial adsorption. A fascinating fact observed is that the electroactive moieties in the compound are getting oxidized and reduced at a potential very close to 0.0 V. The potential of the human body is 0.07 V, so the compound investigated can serve as an efficient candidate for drug delivery.

Declaration of competing interest

The authors declare that they have no known competing financial interests or personal relationships that could have appeared to influence the work reported in this paper.

Acknowledgment

The author and all participants are grateful to the Natural Foundation China (51803081) for the financial support of this work.

The authors would like to thank the Researchers Supporting Project Number (RSP2023R35), King Saud University, Riyadh, Saudi Arabia.

References

Bayol, E., Gürten, A., Dursun, M., Kayakirilmaz, K., 2008. Adsorption behavior and inhibition corrosion effect of sodium carboxymethyl cellulose on mild steel in acidic medium. Acta Phys. Chim. Sin. 24 (12), 2236–2243.

Bhattacharya, S., Bajaj, A., 2009. Advances in gene delivery through molecular design of cationic lipids. Chem. Commun. 31, 4632–4656.

Chauhan, L., Gunasekaran, G., 2007. Corrosion inhibition of mild steel by plant extract in dilute HCl medium. Corros. Sci. 49 (3), 1143–1161.

Connors, T.F., Rusling, J.F., Owlia, A., 1985. Determination of standard potentials and electron-transfer rates for halobiphenyls from electrocatalytic data. Anal. Chem. 57 (1), 170–174.

Fuchs-Godec, R., 2006. The adsorption, CMC determination and corrosion inhibition of some N-alkyl quaternary ammonium salts on carbon steel surface in 2 M H2SO4. Colloids Surf. A Physicochem. Eng. Asp. 280 (1–3), 130–139.

Hu, S., Wu, K., Yi, H., Cui, D., 2002. Voltammetric behavior and determination of estrogens at Nafion-modified glassy carbon electrode in the presence of cetyltrimethylammonium bromide. Anal. Chim. Acta 464 (2), 209–216.

Hu, C., Yang, C., Hu, S., 2007. Hydrophobic adsorption of surfactants on water-soluble carbon nanotubes: a simple approach to improve sensitivity and antifouling capacity of carbon nanotubes-based electrochemical sensors. Electrochem. Commun. 9 (1), 128–134.

Kubesch, P., Boggs, J., Luciano, L., Maass, G., Tuemmler, B., 1987. Interaction of polymyxin B nonapeptide with anionic phospholipids. Biochemistry 26 (8), 2139–2149.

Kumar S. Synthesis and Evaluation of Anti-Corrosive Effect of new Tiourea based Schiff Base towards Steel Corrosion in Acidic Medium.

Melese, A.T., Ayele, D.T., Aljerf, L., Al-Fekaiki, D.F., Akele, M.L., 2023. Investigating the phytoavailability of metals in roots of Croton macrostachyus and Phytolacca dodecandra: induced rhizosphere processes. Biometals 1–13.

Nassar, A.-E., Schenkman, J., Rusling, J., 1997. Direct electron injection from electrodes to cytochrome P450 cam in biomembrane-like films. J. Chem. Soc. Faraday Trans. 93 (9), 1769–1774.

Naveed, A., Li, G., Ali, A., Li, M., Wan, T., Hassan, M., et al., 2023. Realizing high reversibility and safety of Zn anode via binary mixture of Organic solvents. Nano Energy, 108175.

Qureshi, W.A., Haider, S.-N.-U.-Z., Naveed, A., Ali, A., Liu, Q., Yang, J., 2023. Recent progress in the synthesis, characterization and photocatalytic application of energy conversion over single metal atoms decorated graphitic carbon nitride. Int. J. Hydrogen Energy.

Rajeshwar, K., Ibanez, J.G., Swain, G.M., 1994. Electrochemistry and the environment. J. Appl. Electrochem. 24 (11), 1077–1091.

Rasheed, T., Anwar, M.T., Naveed, A., Ali, A., 2022. Biopolymer based materials as alternative greener binders for sustainable electrochemical energy storage applications. ChemistrySelect 7 (39), e202203202.

Rusling, J.F., Nassar, A.E.F., 1993. Enhanced electron transfer for myoglobin in surfactant films on electrodes. J. Am. Chem. Soc. 115 (25), 11891–11897.

Serrano JAS, Llamazares JDM, Timoteo JCC: Electrochemistry of nitroaromatic compounds: From mercury to carbon nanotubes. In: Recent progress on electrochemistry at the Iberian Peninsula: proceeding book of the XL Meeting of the Specialized Group of Electrochemistry of the Royal Spanish Society of Chemistry and the XX Iberian Meeting of Electrochemistry (Huelva, 9th to 12th July 2019). Universidad de Huelva; 2020: 13-6.

Squella, J., Bollo, S., Núñez-Vergara, L., 2005. Recent developments in the electrochemistry of some nitro compounds of biological significance. Curr. Org. Chem. 9 (6), 565–581.

Ullah, I., Shah, A., Badshah, A., Rana, U.A., Shakir, I., Khan, A.M., et al., 2014. Synthesis, characterization and investigation of different properties of three novel thiourea-based non-ionic surfactants. J. Surf. Deterg. 17, 1013–1019.

Ullah, I., Naveed, A., Shah, A., Badshah, A., Khan, G.S., Nadeem, A., 2014. High yield synthesis, detailed spectroscopic characterization and electrochemical fate of novel cationic surfactants. J. Surf. Deterg. 17, 243–251.

Wang, X., Xu, W., Li, Y., Jiang, Z., Zeng, X., Zhang, G., 2023. In-depth unveiling the interfacial adsorption mechanism of triazine derivatives as corrosion inhibitors for carbon steel in carbon dioxide saturated oilfield produced water. J. Colloid Interface Sci. 639, 107–123.

Wu, S.-C., Ai, Y., Chen, Y.-Z., Wang, K., Yang, T.-Y., Liao, H.-J., et al., 2020. High-performance rechargeable aluminum–selenium battery with a new deep eutectic solvent electrolyte: thiourea-AlCl3. ACS Appl. Mater. Interfaces 12 (24), 27064–27073.

Yang, J., Hu, N., Rusling, J.F., 1999. Enhanced electron transfer for hemoglobin in poly (ester sulfonic acid) films on pyrolytic graphite electrodes. J. Electroanal. Chem. 463 (1), 53–62.

Yi, H., Wu, K., Hu, S., Cui, D., 2001. Adsorption stripping voltammetry of phenol at Nafion-modified glassy carbon electrode in the presence of surfactants. Talanta 55 (6), 1205–1210.

Zhang, S., Wu, K., Hu, S., 2002. Voltammetric determination of diethylstilbestrol at carbon paste electrode using cetylpyridine bromide as medium. Talanta 58 (4), 747–754.